Laser and Particle Beams (2007), *25*, 245–252. Printed in the USA.

DOI: 10.1017/S0263034607000080

High resolution X-ray emission spectra from picosecond laser irradiated Ge targets

J. ABDALLAH,[1] D. BATANI,[2] T. DESAI,[2] G. LUCCHINI,[2] A. FAENOV,[3] T. PIKUZ,[3,4] A. MAGUNOV,[3] AND V. NARAYANAN[2]

[1]T-4, Atomic and Optical Physics, Los Alamos National Laboratory, Los Alamos, New Mexico
[2]Dipartimento di Fisica "G.Occhialini", Università di Milano-Bicocca, Milano, Italy
[3]Joint Institute for High Temperature, Russian Academy of Sciences, Moscow, Russia
[4]A.M. Prokhorov General Physics Institute, Russian Academy of Sciences, Moscow, Russia

(RECEIVED 13 October 2006; ACCEPTED 15 February 2007)

Abstract

Investigations of a high resolution X-ray emission spectrum in the range 0.66–0.75 nm obtained by irradiating a Germanium target with high-power p-polarized, 40 picosecond laser radiation at 532 nm wavelength was done. Spectra in the wavelength region of $2l$-$4l'$ and $2l$-$5l'$ L-shell transitions in F-like, Ne-like and Na-like germanium ions were recorded using the FSSR-2D spectrometer equipped with a spherically bent quartz crystal with a spectral resolution $\lambda/\Delta\lambda$ better than 5000. Spectral lines were compared with theoretical values obtained using the LANL plasma kinetic code ATOMIC. Fair agreement between experimental and theoretical spectral lines has been observed, which allowed to measure enough high bulk electron temperature values of 560 eV and electron density of $\sim 10^{21}$ cm^{-3} in Ge plasma irradiated by rather small commercial high repetition rate Nd:YAG laser system.

Keywords: Laser-Plasmas; X-ray spectroscopy; Plasma Diagnostics

1. INTRODUCTION

In recent years, X-rays generated from high-power laser-produced plasmas have gained much importance, and have been applied in several fields including material dynamics (Rousse *et al.*, 2001; Boschetto *et al.*, 2006; Isakov *et al.*, 2005; Schollmeier *et al.*, 2006), radiobiology (Turcu *et al.*, 1994*a*; Bortolotto *et al.*, 2000), the study of fundamental interaction of intense X-rays with matter (Batani *et al.*, 2002), micro-lithography (Turcu *et al.*, 1994*b*), studies of threshold of DNA damage (Turcu *et al.*, 1994*a*), of radiation induced damage to cell metabolism (Masini *et al.*, 1999; Milani *et al.*, 1999), water-window X-ray microscopy (Batani *et al.*, 2000; Desai *et al.*, 2003, 2004; Poletti *et al.*, 2004), diagnostics of laser produced plasmas i.e., determination of plasma density and temperature (Koenig *et al.*, 1997; Magunov *et al.*, 1998; Batani *et al.*, 1999; Pisani *et al.*, 1999; Adamek *et al.*, 2006; Korobkin *et al.*, 2005; Kawamura *et al.*, 2006), identification of atomic processes (Stepanov *et al.*, 1997; Rosmej *et al.*, 1997; Biemont *et al.*, 2000), etc.

Recently, back-lighters with high photon energies are being developed in order to access the hot and dense regions of laser produced plasmas. In this context, Ge back lighters and Ge X-ray lasers have been applied (Da Silva *et al.*, 1993, 1995; Celliers *et al.*, 1997; Bennett, 2001; Kalantar *et al.*, 1996).

Also, Ge targets have been used as one of the first lasing medium in X-ray laser experiments, and nowadays, Ge targets are still one of the main approaches to X-ray lasers. Gain studies and accurate wavelength measurement of lasing have been investigated (Enright *et al.*, 1991; Rosen *et al.*, 1985; Zhang *et al.*, 1996; Warwick *et al.*, 1998; Burge *et al.*, 1997; Lewis *et al.*, 1992; Kodama *et al.*, 1994; Yuan *et al.*, 1996; Mocek *et al.*, 2005).

For all these reasons, an accurate determination of Ge X-ray spectrum is important, as well as understanding its variations, as results of the changes in the laser/plasma parameters. In the present work, we have studied X-ray spectra obtained by irradiating a flat Ge target with a ps-duration Nd:YAG laser system (Faenov *et al.*, 2004; Batani *et al.*, 2005). X-ray emission spectra have been recorded using the

Address correspondence and reprint requests to: D. Batani, Dipartimento di Fisica "G.Occhialini", Università di Milano-Bicocca, Piazza della Scienza 3, 20126 Milano, Italy. E-mail: batani@mib.infn.it

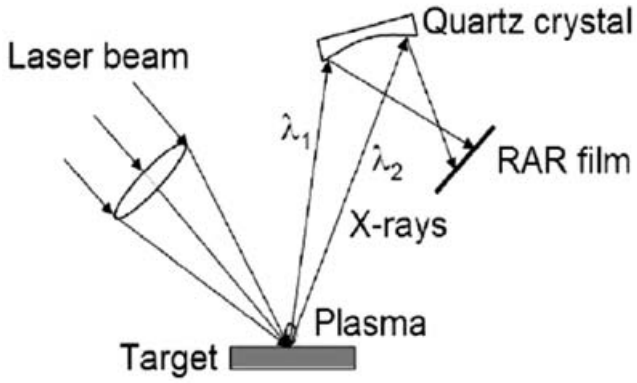

Fig. 1. Experimental setup of the X-ray spectra measurements of the laser plasma emission by the FSSR-2D spectrometer based on the spherically bent quartz crystal.

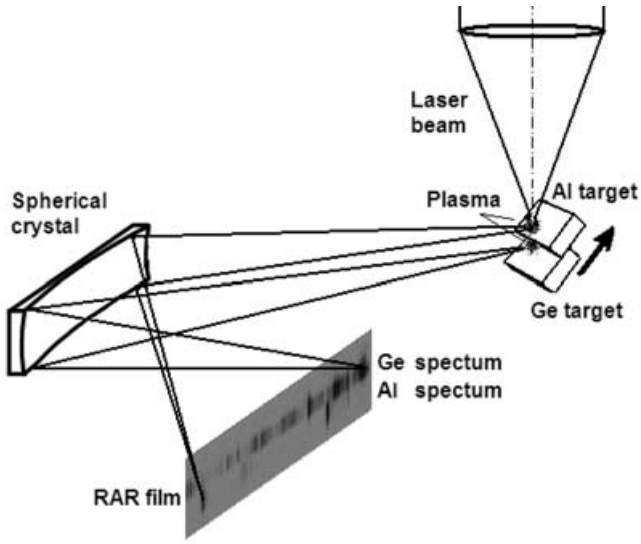

Fig. 2. The optical scheme of spatially resolved (in the vertical direction) X-ray spectra recorded by the FSSR spectrometer with a spherically bent quartz crystal.

focusing spectrometer with spatial resolution-two-dimensional (FSSR-2D) high-resolution spectrometer and using RAR X-ray films. As discussed in Faenov *et al.* (2004) and Magunov *et al.* (2006), the very small focal spot which can be obtained using such a laser system, as well as its short pulse duration, limits the plasma size (i.e., the X-ray source size), and therefore allows maintaining the high spectral resolution of the spectrometer. Experimental results have been compared to calculations performed using the Los

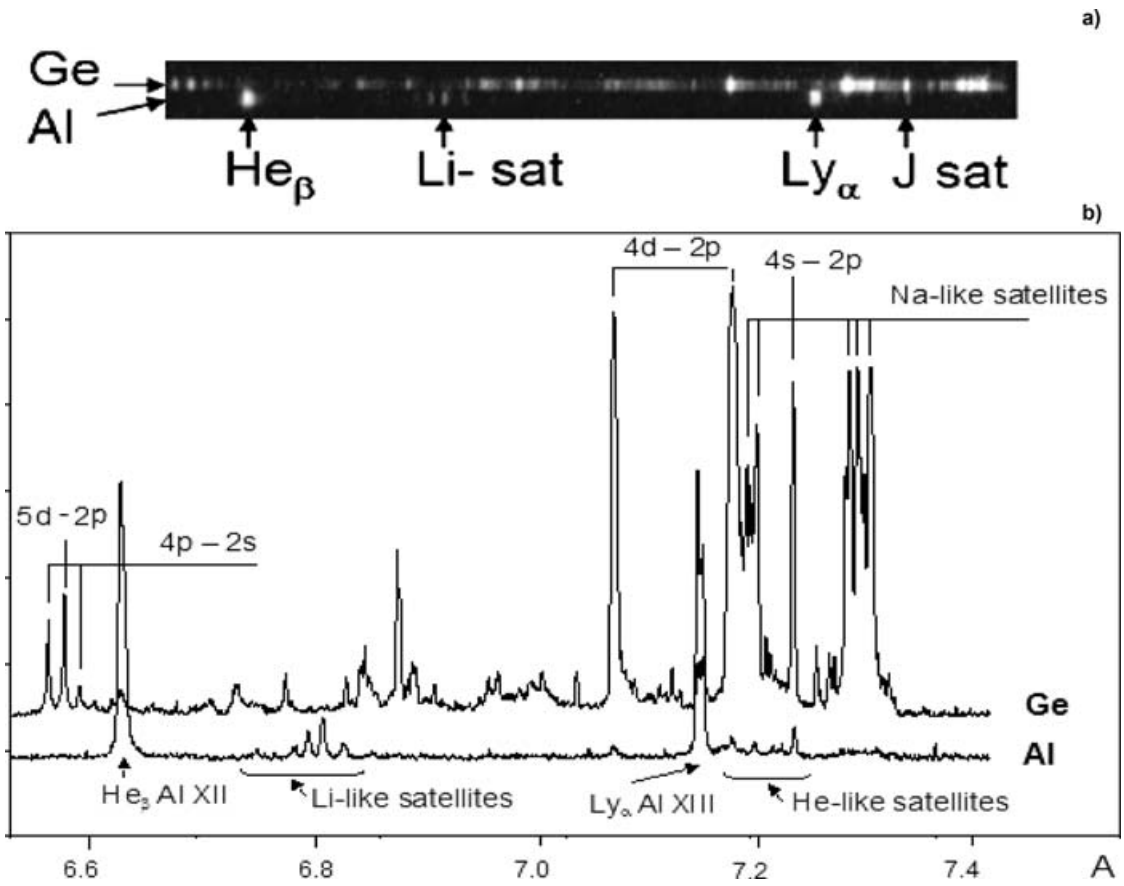

Fig. 3. (**a**) The RAR film image with the spectra of Ge and Al plasmas recorded on in the 6.5–7.4 Å wavelength range. (**b**) The optical density (in arbitrary units) of experimentally observed X-ray spectra of the Ge and Al plasmas.

https://doi.org/10.1017/S0263034607000080 Published online by Cambridge University Press

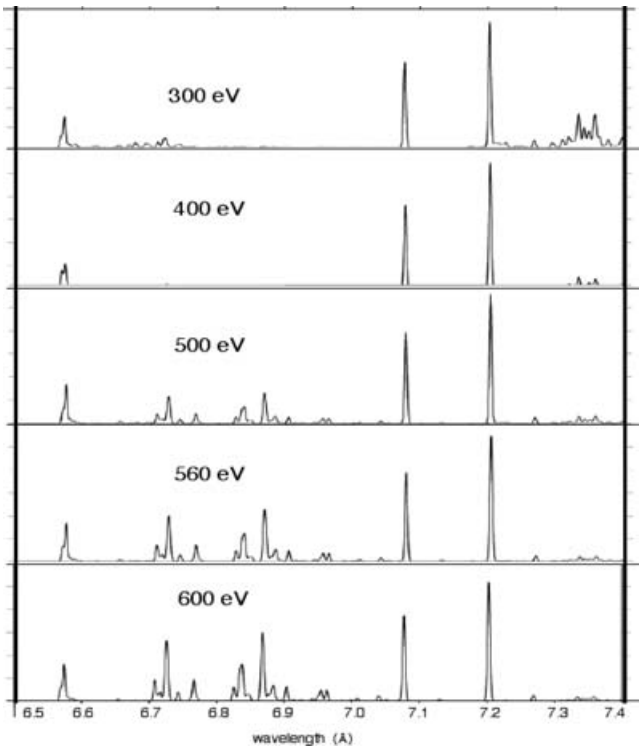

Fig. 4. The X-ray spectral lines of the F-like, Ne-like, and Na-like Ge ions. A simplified kinetic model calculation at the electron density $n_e = 10^{21}$ cm^{-3} and different electron temperature values.

Alamos National Laboratory (LANL) plasma kinetic code ATOMIC and a general agreement has been obtained.

2. EXPERIMENTAL SETUP

Experiments were performed at the University of Milano-Bicocca using an Nd: YAG laser system capable of delivering up to 120 mJ in 40 ps (FWHM) linearly *p*-polarized 1064 nm laser radiation, which can be operated from 1 to 10 Hz repetition rate. In the present experiment, the laser frequency was up-converted to the second harmonic 532 nm using KD*P crystal. Details of the laser system are described in Faenov *et al.* (2004). The laser radiation was focused on a spot radius of 12 μm on a planar 100 μm thick Ge target at an angle of 45° to the target normal with a condition of the *p*-polarization. Experimental arrangement is shown in Figure 1.

The target surface was adjusted in the lens focal plane by maximizing the X-ray signal measured by two Silicon PIN diodes. These diodes were covered with two-layers of polypropylene foils, each of 1 μm thickness, coated with 0.2 μm of Al. In this experiment, laser energy per shot was nearly constant $E_L \approx 20$ mJ corresponding to laser intensity on the target surface $I_L \approx 10^{14}$ W/cm^2. The interaction chamber was evacuated to a residual pressure of $p \approx 10^{-3}$ torr.

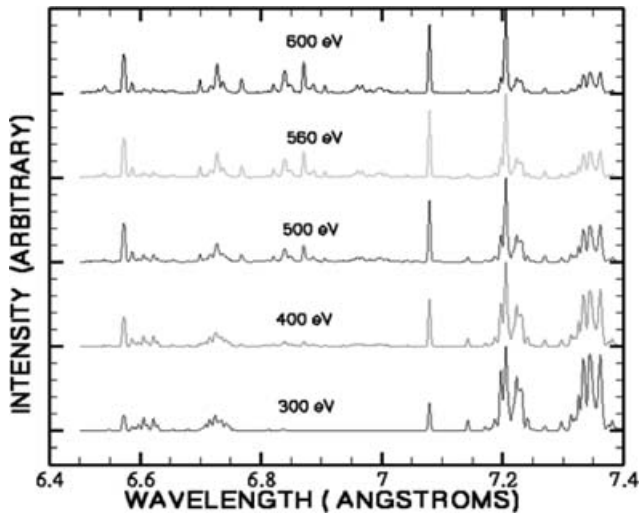

Fig. 5. The full model calculations for the electron density $n_e = 10^{21}$ cm^{-3} and different values of the electron temperature.

3. HIGH-RESOLUTION SPECTROMETER

High-resolution spectra were recorded using the FSSR in the 2D scheme (Faenov *et al.*, 1994; Pikuz *et al.*, 1995; Young *et al.*, 1998) as shown in Figure 2. The spectrometer was equipped with a spherically bent quartz crystal with the curvature radius $R = 100$ mm and the distance between symmetric planes $2d = 0.85$ nm (Alexandropoulos & Cohen, 1974; Holzer *et al.*, 1998)

X-ray emission from the Ge plasma in the 0.65–0.74 nm spectral range was recorded. The choice of the crystal enabled to record the emission from $n = 4 - n' = 2$ transition in Ne-like and F-like Ge ions. The spectral magnification was 1:1 with the spatial resolution $\delta x \approx 15$ μm. The effective spectral resolution $\lambda/\Delta\lambda$ was better than 5000 in the present experiment. The spectrometer was placed at the angle 70° to the laser axis and RAR-2492 film was used to record the X-ray emission spectra. A 2-μm thick C_3H_6 film coated with 0.4 μm Al on both sides was used as a filter to cut-off the visible and VUV radiation from exposing the RAR film. Due to small laser pulse energy, it was necessary to accumulate about 130 laser shots on the Ge target to record reasonably good spectra on the RAR-2492 film. After each shot, the damaged target was shifted in its plane.

We have recorded on the same film the $1s3p\ ^{1,3}P_1 - 1s^2\ ^1S$ line of the He-like Al ion and the Ly_α line of the H-like Al ion together with their dielectronic satellites. This was achieved using the spatial resolution of the FSSR-2D spectrometer. The Al target was placed in the interaction chamber at a position, which was shifted about 0.5 mm in respect to the Ge-target in the direction perpendicular to the X-ray reflection plain (Fig. 2). Thus, the well-known Al spectral lines were used as accurate wavelength references for the Ge lines. The recorded spectra were scanned and transformed into the optical density plot and finally into the intensity

https://doi.org/10.1017/S0263034607000080 Published online by Cambridge University Press

Table 1. *Transition lines (angstroms)*

	Theory	Experiment
1s) 1s 0.0 2s2 2p6 – 2p) 1p 1.0 2s2 2p5 5d1	6.5717	6.5754
1s) 1s 0.0 2s2 2p6 – 2s) 1p 1.0 2s1 2p6 4p1	6.5744	6.5883
2p) 2p 1.5 2s2 2p6 3p1 – 3p) 2d 2.5 2s2 2p5 3p1 5d1	6.6060	6.6008
2p) 2p 0.5 2s2 2p6 3p1 – 3d) 4f 1.5 2s2 2p5 3p1 5d1	6.6126	6.6120
2d) 2d 2.5 2s2 2p6 3d1 – 3p) 2f 3.5 2s2 2p5 3d1 5d1	6.6223	6.6268
1s) 1s 0.0 2s2 2p6 – 2p) 1p 1.0 2s2 2p5 5s1	6.6548	6.6597
2p) 2p 0.5 2s2 2p5 – 1s) 2d 1.5 2s2 2p4 4d1	6.6993	6.7031
2s) 2s 0.5 2s2 2p6 3s1 – 1p) 2p 1.5 2s2 2p5 3s1 5d1	6.7087	6.7077
2p) 2p 1.5 2s2 2p5 – 1d) 2s 0.5 2s2 2p4 4d1	6.7294	6.7324
2p) 2p 1.5 2s2 2p5 – 1d) 2p 1.5 2s2 2p4 4d1	6.7282	
2p) 2p 1.5 2s2 2p5 – 1d) 2f 2.5 2s2 2p4 4d1	6.7261	
2s) 2s 0.5 2s1 2p6 – 1p) 2p 0.5 2s1 2p5 4d1	6.7367	6.7444
2s) 2s 0.5 2s1 2p6 – 1p) 2p 1.5 2s1 2p5 4d1	6.7391	
2p) 2p 1.5 2s2 2p5 – 3p) 2f 2.5 2s2 2p4 4d1	6.7679	6.7739
2p) 2p 1.5 2s2 2p5 – 3p) 4p 2.5 2s2 2p4 4d1	6.7694	6.7791
2p) 3d 2.0 2s2 2p5 3p1 – 1s) 1f 3.0 2s2 2p4 3p1 4d1	6.8124	6.8048
2p) 2p 1.5 2s2 2p5 – 1s) 2d 2.5 2s2 2p4 4d1	6.8212	6.8227
2p) 2p 0.5 2s2 2p5 – 1d) 2d 1.5 2s2 2p4 4d1	6.8405	6.8408
2s) 2s 0.5 2s1 2p6 – 3p) 4f 1.5 2s1 2p5 4d1	6.8470	6.8502
2p) 2p 1.5 2s2 2p5 – 3p) 2d 2.5 2s2 2p4 4d1	6.8701	6.8755
2p) 2p 1.5 2s2 2p5 – 3p) 2p 0.5 2s2 2p4 4d1	6.8792	6.8845
2p) 2p 0.5 2s2 2p5 – 3p) 2p 1.5 2s2 2p4 4d1	6.8870	6.8887
2s) 2s 0.5 2s1 2p6 – 3p) 2p 1.5 1s2 2s1 2p5 4d1	6.9058	6.9091
2s) 2s 0.5 2s1 2p6 – 3p) 2p 0.5 2s1 2p5 4d1	6.9591	6.9609
2s) 2s 0.5 2s1 2p6 – 3p) 2d 1.5 2s1 2p5 4d1	6.9675	6.9705
2p) 1s 0.0 2s2 2p5 3p1 – 1d) 1p 1.0 2s2 2p4 3p1 4d1	6.9789	6.9789
2p) 3d 2.0 2s2 2p5 3p1 – 3p) 3d 2.0 2s2 2p4 3p1 4d1	7.0001	7.0011
2s) 3s 1.0 2s1 2p6 3s1 – 4p) 3p 2.0 2s1 2p5 3s1 4d1	7.0088	7.0122
2p) 2p 1.5 2s2 2p5 – 3p) 2p 1.5 2s2 2p4 4s1	7.0419	7.0402
1s) 1s 0.0 2s2 2p6 – 2p) 3d 1.0 2s2 2p5 4d1	7.0789	7.0845
2p) 2p 0.5 2s2 2p6 3p1 – 1s) 2d 1.5 2s2 2p5 3p1 4d1	7.1424	7.1445
2p) 2p 1.5 2s2 2p6 3p1 – 1s) 2d 2.5 2s2 2p5 3p1 4d1	7.1712	7.1762
1s) 1s 0.0 2s2 2p6 – 2p) 1p 1.0 2s2 2p5 4d1	7.2050	7.2078
2d) 2d 2.5 2s2 2p6 3d1 – 3p) 2f 3.5 2s2 2p5 3d1 4d1	7.2236	7.2229
2d) 2d 2.5 2s2 2p6 3d1 – 3d) 4d 3.5 2s2 2p5 3d1 4d1	7.2285	7.2274
2d) 2d 2.5 2s2 2p6 3d1 – 1d) 2d 2.5 2s2 2p5 3d1 4d1	7.2322	7.2333
2d) 2d 1.5 2s2 2p6 3d1 – 3f) 2d 1.5 2s2 2p5 3d1 4d1	7.2409	7.2445
1s) 1s 0.0 2s2 2p6 – 2p) 3p 1.0 2s2 2p5 4s1	7.2698	7.2727
2p) 2p 1.5 2s2 2p6 3p1 – 3p) 4d 2.5 2s2 2p5 3p1 4d1	7.2970	7.2999
2d) 2d 1.5 2s2 2p6 3d1 – 1p) 2d 2.5 2s2 2p5 3d1 4d1	7.3133	7.3130
2d) 2d 2.5 2s2 2p6 3d1 – 1p) 2d 2.5 2s2 2p5 3d1 4d1	7.3193	7.3183
2p) 2p 0.5 2s2 2p6 3p1 – 3d) 4p 1.5 2s2 2p5 3p1 4d1	7.3374	7.3362
2d) 2d 2.5 2s2 2p6 3d1 – 3d) 2f 3.5 2s2 2p5 3d1 4d1	7.3464	7.3448
2d) 2d 2.5 2s2 2p6 3d1 – 3d) 2d 2.5 2s2 2p5 3d1 4d1	7.3603	7.3588
2d) 2d 1.5 2s2 2p6 3d1 – 1d) 2p 1.5 2s2 2p5 3d1 4d1	7.3751	7.3728
2d) 2d 2.5 2s2 2p6 3d1 – 3f) 2d 2.5 2s2 2p5 3d1 4d1	7.3823	7.3801

plot by using standard density and intensity calibration curves. The image of the original film and its densitometry are shown in Figure 3.

4. THE SIMULATION CODE

In order to analyze the high-resolution Ge X-ray spectrum recorded by the FSSR-2D spectrometer, we used the LANL suite of atomic physics codes. In the wavelength range from 0.66 to 0.74 nm, the prevalent emission is from the $n = 4–n' = 2$ transitions in the Na-like, Ne-like, and F-like Ge ions.

The code modeled O-like, F-like, Ne-like, Na-like, and Mg-like ionization stages of the Ge atom. The atomic model used for this calculation includes a few 100 configurations in each of the ionization stages cited above. For example, the Ne-like Ge includes $1s^22s^22p^6$, $1s^22s^22p^5nl$, $1s^22s^22p^43snl$, $1s^22s^22p^43pnl$, $1s^22s^22p^6nl$, $1s^22s^22p^53snl$, $1s^22s^22p^53pnl$, $1s^22p^63snl$, and $1s^22p^63pnl$ configurations. Here, configurations with the principal quantum number through $n = 7$ and the orbital momentum quantum number through $l = 6$ were considered. Similar configuration sets were specified for the O-like, F-like, Na-like, and Mg-like ions.

The CATS code (Abdallah *et al.*, 1998) based on the atomic physics programs of Cowan (1981) was used to calculate the atomic structure including energy levels, and radiative transition probabilities. The electron impact excitation cross sections were calculated by the ACE code (Clark *et al.*, 1988) in the distorted-wave approximation. The GIPPER code (Abdallah *et al.*, 2001) was used to calculate cross sections for electron impact ionization, photon induced ionization, and auto-ionization between appropriate states in adjacent ion stages.

The obtained set of atomic structure and cross section data was used in the ATOMIC code (Hakel *et al.*, 2006) to simulate the experimentally observed spectra. A configuration average model was used to calculate the configuration populations by solving the steady-state rate equations using the full complement of atomic processes for the configurations discussed above. The fine structure populations of the levels N_{cJ} with the total angular momentum quantum number, J, were obtained by a statistical distributing of corresponding configuration populations, N_c, obtained from the solution of the rate equations:

$$N_l = (2j + 1)N_c/g_c, \quad (1)$$

where g_c is the configuration statistical weight.

A more accurate solution of the kinetic problem follows from the level rate equation set. However, in our case, about 70000 levels resulted from the considered configurations, which make the direct calculations almost impracticable in time.

Finally, the resulting level populations (Eq. 1) and corresponding transition probabilities were then used to construct the line emission spectra.

5. RESULTS AND DISCUSSION

Figure 3 shows the experimentally observed X-ray spectra (optical density, arb. units) from Al and Ge plasmas. The Ge spectrum clearly shows the lines corresponding to the $4l–2l'$ transitions representing to the Na-like and Ne-like ions.

Figure 4 shows the simulated spectra obtained for Ge plasma. These calculations were made for the electron

https://doi.org/10.1017/S0263034607000080 Published online by Cambridge University Press

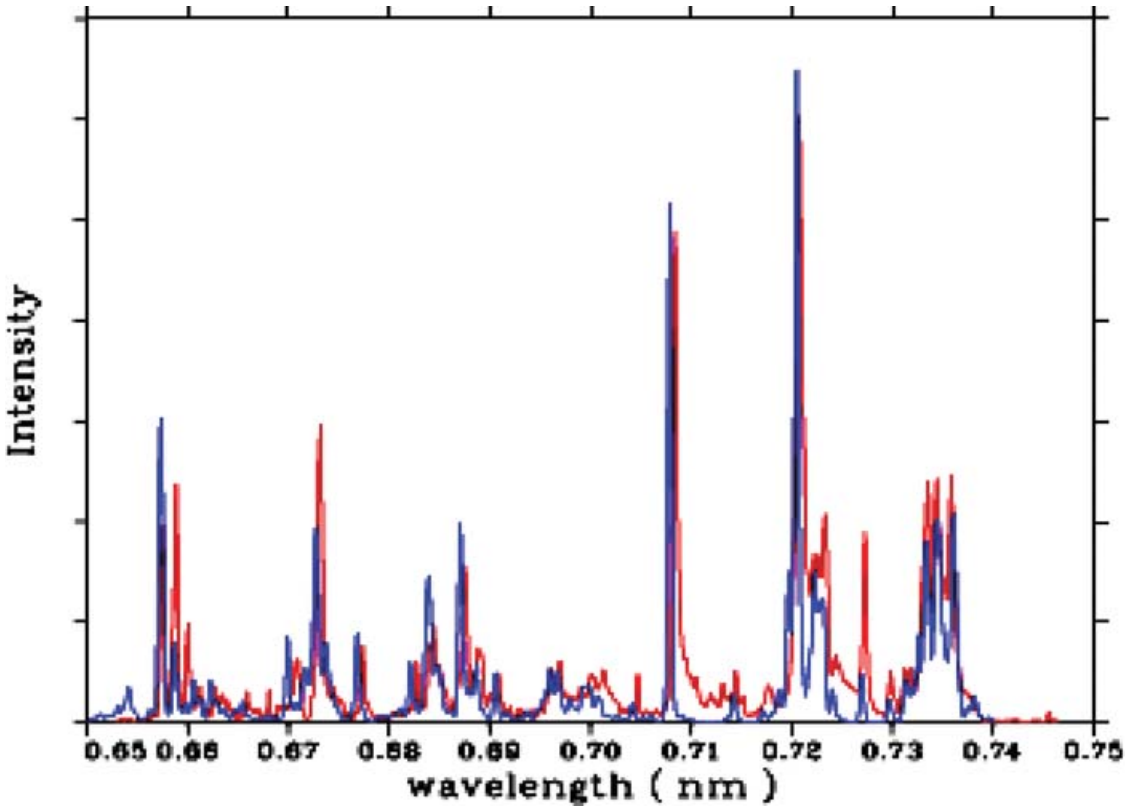

Fig. 6. Comparison of the calculated spectrum (blue curve) with experimental data (red curve).

density $n_e = 10^{21}$ cm^{-3}, and varying temperature 300, 400, 500, 560, and 600 eV. Calculated spectra have been obtained with a simplified model just in order to see the changes induced by the temperature variation. Only F-, Ne-, and Na-like ions are considered through $n = 5$. Not many auto-ionizing levels are included, implying that the real plasma should probably be more recombining. Although the Born cross sections are pretty crude, the main spectral features are accounted for. Figure 5 shows instead the same spectra calculated for the electron density $n_e = 10^{21}$ cm^{-3}, and varying the temperature, but using the full model.

Table 1 shows the data of transition and the calculated values of X-ray wavelengths along with experimental values for comparison. We notice that in general, the agreement is quite good. It shows that our laser system together with the FSSR-2D spectrometer can be used for accurate wavelength measurements. For several observed spectral structures, many lines are overlapping and we have listed the most dominant one. For a few cases, there was no dominant line in the group, so we listed them all. We didn't include lines that we had low confidence in.

Figure 6 shows a comparison of the experimental spectrum with a spectrum calculated for an electron temperature of 560 eV and electron density of 10^{21} cm^{-3}, parameters for which we get the best agreement between experiment and calculation. Here the experimental spectrum has been converted to relative X-ray intensities by using standard film sensitivity, crystal reflectivity, and filter transmissivity (Henke *et al.*, 1984, 1986; Henke & Jaanimagi, 1985; Holzer *et al.*, 1998).

Opacity effects are included by using escape factors for spectral lines that correspond to a plasma size of about 20 μm. Note that in general, the agreement is very good, however, the relative intensities for some spectral lines are not in agreement. This could be due to optical depth effects which depend on the plasma size and electron impact cross section. However, it is more likely due to the fact that configuration based kinetics rather than detailed level-to-level kinetics is used, leading to discrepancy in level populations.

Let's finally notice that, on the basis of simple analytical models (Max, 1982), which are however usually well compared to experiments, we do expect, in our conditions, a plasma temperature, T_e, of about 1 keV in the critical region ($n_e \approx 4 \times 10^{21}$ cm^{-3} due to frequency doubling). However, in our case, the focal spot radius is very small (about 12 μm as was said before). Hence, 2D effects are expected to be important in plasma expansion causing a reduced density and plasma cooling. Therefore, we can conclude that the values of $T_e = 560$ eV and $n_e = 10^{21}$ cm^{-3} estimated from the measurement compare well with expectations.

https://doi.org/10.1017/S0263034607000080 Published online by Cambridge University Press

6. CONCLUSIONS

We have performed high-precision X-ray spectroscopy studies of Ge plasmas produced by irradiating 100 μm thick Ge target with 40 ps laser radiation at 532 nm wavelength from a small, commercial, high-repetition rate Nd:YAG laser system, which delivered the intensity on the target surface $\sim 10^{14}$ W/cm^2. X-ray emission spectra in the spectral range from 0.65 to 0.74 nm were recorded using the spherically bent quartz crystal spectrometer. The measured wavelength and intensities of experimentally observed spectral lines were compared with theoretical values obtained using LANL opacity and plasma kinetic code ATOMIC. Calculated line intensities are in good agreement with experimental data at the electron density $n_e \approx 10^{21}$ cm^{-3} and temperature $T_e \approx 560$ eV. The results of spectral measurements manifest that laser-produced plasmas obtained in our experiment seem to be promising point- bright source of soft X-ray radiation.

ACKNOWLEDGEMENTS

We acknowledge the support of the Italian Program FISR Legge 449/97 "Impianti innovativi multiscopo per la produzione di radiazione X e ultravioletta, coerente ed incoerente ad alta intensità". A.M. is grateful for hospitality of the University Milano Bicocca and for the support of the Consorzio Nazionale Interuniversitario per le Scienze Fisiche della Materia according to the Contract FOES000040. This work was also performed under the auspices of the US Department of Energy.

REFERENCES

Abdallah, J., Jr., Clark, R.E.H. & Cowan, R.D. (1998). Theoretical Atomic Physics Code Development I - CATS: Cowan Atomic Structure Code, LA-11436-M, vol. I, Manual UC-705.

Abdallah, J., Jr., Zhang, H.L., Fontes, C.J., Kilcrease, D.P. & Archer, B.J. (2001). Model comparisons for high-Z non-LTE steady-state calculations. *JQSRT* **71**, 107–116.

Adamek, P., Renner, O., Drska, L., Rosmej, F.B. & Wyart, J.F. (2006). Genetic algorithms in spectroscopic diagnostics of hot dense plasmas. *Laser Part. Beams* **24**, 511–518.

Alexandropoulos, N.G. & Cohen, G.G. (1974). Crystals for stellar spectrometers. *Appl. Spec.* **28**, 155–164.

Batani, D., Botto, C., Bortolotto, F., Masini, A., Bernardinello, A., Moret, M., Poletti, G., Cotelli, F., Lora Lamia Donin, C. Piccoli, S., Stead, A., Ford, T., Marranca, A., Eidmann, K., Flora, F., Palladino, L. & Reale, L. (2000). Contact X-ray microscopy using the Asterix laser source. *Phys. Medica* **14**, 49

Batani, D., Desai, T., Löwer, T.H., Hall, T.A., Nazarov, W., Koenig, M. & Benuzzi-Mounaix, A. (2002). Interaction of soft X-ray thermal radiation with foam layered targets. *Phys. Rev. E* **65**, 066404.

Batani, D., Desai, T., Lucchini, G., Canova, F., Magunov, A.I., Faenov, A.Ya., Pikuz, T.A., Skobelev, I.Yu. & Chiodini, N. (2005). Generation and characterization of a bright x-ray source using picosecond laser. *Rad. Effects Defects Solids* **160**, 507–514.

Batani, D., Koenig, M., Benuzzi, A., Boudenne, J.M., Cauchon, G., Hall, T. & Nazarov, W. (1999). X-ray diagnostic applied to the study of shock wave propagation in foams. *Rev. Sci. Instr.* **70**, 1464–1467.

Bennett, G.R. (2001). Advanced laser-backlit grazing-incidence X-ray imaging systems for inertial confinement fusion research. I. Design. *Appl. Opt.* **40**, 4570–4587.

Biemont, E., Magunov, A.I., Dyakin, V., Faenov, A., Pikuz, T., Skobelev, I., Osterheld, A., Goldstein, W., Flora, F., Di Lazzaro, P., Bollanti, S., Lisi, N., Letardi, T., Reale, A., Palladino, L., Batani, D., Mauri, A., Scafati, A. & Reale, L. (2000). Measurement of the ground state ionisation energy and wavelengths for the 2l-nl′ transitions of Ni XIX ($n = 4–14$) and Ge XXIII ($n = 7–9$). *J. Phys. B: At. Mol. Opt. Phys.* **33**, 2153–2162.

Bortolotto, F., Batani, D., Masini, A., Previdi, F., Rebonato, L. & Turcu, E. (2000). Study of a X-ray laser-plasma source for radiobiological experiments, microdosimetry analysis and plasma characterization. *Euro. Phys. J. D* **11**, 309.

Boschetto, D., Gamaly, E.G., Rode, A.V., Glijer, D., Garl, T., Albert, O., Rousse, A. & Etchepare, J. (2006). Reflectivity oscillations of fs-laser excited Bismuth: excitation of coherent phonons. In *High-Power Laser Ablation VI* (C.R. Phipps, Ed.). Bellingham WA: SPIE.

Burge, R.E., Slark, G.E., Browne, M.T., Yuan, X.-C., Charalambous, P., Cheng, X.-H., Lewis, C.L.S., MacPhee, A. & Neely, D. (1997). Spatial coherence of x-ray laser emission from neonlike germanium after prepulse. *J. Opt. Soc. Am. B* **14**, 2742.

Celliers, P., Barbee Jr. T.W., Cauble, R., Da Silva, L.B., Decker, C.D., Kalantar, D.H., Key, M.H., London, R.A., Moreno, J.C., Snavely, R., Trebes, J.E., Wan, A.S. & Weber, F. (1997). Probing high density plasmas with soft x-ray lasers. UCRL-JC—126541. http://www.osti.gov/bridge/servlets/purl/16525-7gWT6S/native/16525.PDF.

Clark, R.E.H., Abdallah, J., Csanak, G., Mann, J.B. & Cowan, R.D. (1988). ACE: Another Collisional Excitation Code. LA-11436-M. Los Alamos, NM: Los Alamos National Laboratoy.

Cowan, R.D. (1981). *Theory of Atomic Structure and Spectra*. Berkeley: University of California Press.

Da Silva, L.B., Barbee, T.W., Jr., Cauble, R., Celliers, P., Ciarlo, D., Libby, S., London, R.A., Matthews, D., Mrowka, S., Moreno, J.C., Ress, D., Trebes, J.E., Wan, A.S. & Weber, F. (1995). Electron density measurements of high density plasmas using soft x-ray laser interferometry. *Phys. Rev. Lett.* **74**, 3991–3994.

Da Silva, L.B., Cauble, B., Frieders, G., Koch, J.A., MacGowan, B.J., Matthews, D.L., Mrowka, S., Ress, D., Trebes, J.E. & Weiland, T.L. (1993). Imaging with x-ray lasers. UCRL-JC—114478. Bellingham WA: SPIE.

Desai, T., Batani, D., Bernardinello, A., Poletti, G., Orsini, F., Ullschmied, J., Juha, L., Skala, J., Kralikova, B., Krousky, E., Pfeifer, M., Kadlec, C., Mocek, T., Präg, A., Renner, O., Cotelli, F., Lamia, C.L. & Zullini, A. (2003). X-ray microscopy of living multi-cellular organisms with PALS. *Laser Part. Beams* **21**, 509–514.

Desai, T., Batani, D., Bernardinello, A., Poletti, G., Orsini, F., Ullschmied, J., Skala, J., Kralikova, B., Krousky, E., Pfeifer, M., Kadlec, Ch., Mocek, T., Präg, A., Renner, O., Juha, L., Cotelli, F., Lamia, C.L. & Zullini, A. (2004). Investigations of *Caenorhabditis elegans* using soft X-ray contact microscopy. *Phys. Medica* **XX**, 3.

Enright, G.D., Villeneuve, D.M., Dunn, J., Baldis, H.A., Kieffer, J.C., Pepin, H., Chaker, M. & Herman, P.R. (1991). X-ray laser gain measurements in a collisionally excited germanium plasma. *J. Opt. Soc. Am. B: Opt. Phys.* **8**, 2047–2052.

Faenov, A., Magunov, A., Pikuz, T., Batani, D., Lucchini, G., Canova, F. & Piselli, M. (2004). Bright, point X-ray source based on a commercial portable 40 ps Nd YAG laser system. *Laser Part. Beams* **22**, 373–379.

Faenov, A.Y.A., Pikuz, S.A., Erko, A.I., Bryunetkin, B.A., Dyakin, V.M., Ivanenkov, G.V., Mingaleev, A.R., Pikuz, T.A., Romanova, V. & Shelkovenko, T.A. (1994). High performance X-ray spectroscopic devices for plasma microsources investigations. *Phys. Scripta* **50**, 333.

Hakel, P., Sherrill, M.E., Mazevet, S., Abdallah, J., Jr., Colgan, J., Kilcrease, D.P., Magee, N.H., Fontes, C.J. & Zhang, H.L. (2006). The new Los Alamos opacity code ATOMIC. *J. Quan. Spectr. Rad. Tran.* **99**, 265–271.

Henke, B.L, Uejio, J.Y., Stone, G.F., Dittmore, C.H. & Fujiwara, F.G. (1986). High-energy x-ray response of photographic films: Models and measurement. *J. Opt. Soc. Am. B* **3**, 1540–1550.

Henke, B.L. & Jaanimagi, P.A. (1985). Two-channel, elliptical analyzer spectrograph for absolute, time-resolving time-integrating spectrometry of pulsed X-ray sources in the 100–10000-ev region. *Rev. Sci. Instrum.* **56**, 1537–1552.

Henke, B.L., Kwok, S.L., Uejio, J.Y., Yamada, H.T. & Young, G.C. (1984). Low-energy X-ray response of photographic films. I. Mathematical models. *J. Opt. Soc. Am. B* **1**, 818–827.

Holzer, G., Wehrhan, O. & Forster, E. (1998). Characterization of flat and bent crystals for x-ray spectroscopy and imaging. *Cryst. Res. Technol.* **33**, 555.

Isakov, V.A., Kanavin, A.P. & Uryupin, S.A. (2005). Reflection and absorption of a high-power ultrashort laser pulse heating a solid-state target. *Laser Part. Beams* **23**, 315–319.

Kalantar, D.H., Haan, S.W., Hammel, B.A., Keane, C.J., Landen, O.L. & Munro, D.H. (1996). Measurement of the in-flight pusher density of an indirect drive capsule implosion core using x-ray backlighting. http://www.osti.gov/energycitations/servlets/purl/250565d7JCh6/webviewable/250565.pdf

Kawamura, T., Horioka, K. & Koike, F. (2006). Potential of K alpha radiation by energetic ionic particles for high energy density plasma diagnostics. *Laser Part. Beams* **24**, 261–267.

Kodama, R., Neely, D., Kato, Y., Daido, H., Murai, K., Yuan, G., MacPhee, A. & Lewis, C.L.S. (1994). Generation of small-divergence soft X-ray laser by plasma wave guiding with a curved target. *Phys. Rev. Lett.* **73**, 3215–3218.

Koenig, M., Boudenne, J.M., Legriel, P., Grandpierre, T., Batani, D., Bossi, S., Nicolella, S. & Benattar, R. (1997). A computer driven crystal spectrometer with CCD detectors for X-ray spectroscopy of laser-plasmas. *Rev. Sci. Instrum.* **68**, 2387–2392.

Korobkin, Y.V., Romanov, I.V., Rupasov, A.A., Shikanov, A.S., Gupta, P.D., Khan, R.A., Kumbhare, S.R., Moorti, A. & Naik, P.A. (2005). Hard X-ray emission in laser-induced vacuum discharge. *Laser Part. Beams* **23**, 333–336.

Lewis, C.L.S., Neely, D., O'Neill, D.M., Uhomoibhi, J.O., Key, M.H., Al Hadithi, Y., Tallents, G.J. & Ramsden, S.A. (1992). An injector/amplifier double target configuration for the Ne-like Ge X-ray laser scheme. *Opt. Commun.* **91**, 71–76.

Magunov, A., Batani, D., Faenov, A.Ya., Lucchini, G., Desai, T., Padoan, F., Pikuz, T.A., Skobelev, I.Yu., Canova, F. & Chiodini, N. (2006). Characterization of compact bright soft X-ray source based on picosecond laser plasma. *Appl. Phys. B: Lasers Opt.* **82**, 19–24.

Magunov, A., Faenov, A., Skobelev, I., Pikuz, T., Batani, D., Milani, M., Costato, M., Pozzi, A., Turcu, E., Allot, R., Koenig, M., Benuzzi, A., Flora, F. & Reale, A. (1998). Formation of the X-ray line emission spectrum of excimer laser-produced plasmas. *Laser Part. Beams* **16**, 61–70.

Masini, M., Batani, D., Previdi, F., Costato, M., Pozzi, A., Turcu, E., Allott, R. & Lisi, N. (1999). Yeast cell metabolism investigated by CO_2 production and soft X-ray irradiation. *Euro. Phys. J.: Appl. Phys.* **5**, 101–109.

Max, C.E. (1982). Physics of the coronal plasma in laser fusion targets. In *Laser-Plasma Interactions* (R. Balian R. & Adam J.C., Eds.). Amsterdam: North Holland.

Milani, M., Conte, A., Costato, M., Salsi, F., Baroni, G., Batani, D., Ferrario, L. & Turcu, E. (1999). NMR and pressure correlated analysis of metabolic changes in soft X-rays irradiated yeast cells. *Euro. Phys. J. D* **5**, 267–270.

Mocek, T., Sebban, S., Bettaibi, I., Zeitoun, P., Faivre, G., Cros, B., Maynard, G., Butler, A., McKenna, C.M., Spence, D.J., Gonsavles, A., Hooker, S.M., Vorontsov, V., Hallou, S., Fajardo, M., Kazamias, S., Le Pape, S., Mercere, P., Morlens, A.S., Valentin, C. & Balcou, P. (2005). Progress in optic-field-ionization soft X-ray lasers at LOA. *Laser Part. Beams* **23**, 351–356.

Pikuz, T.A., Faenov, A., Pikuz, S., Romanova, V.M. & Shelkovenko, T.A. (1995). Bragg X-ray optics for imaging spectroscopy of plasma microsources. *J. X-Ray Sci. Technol.* **5**, 323.

Pisani, F., Koenig, M., Batani, D., Hall, T., Desenne, D., Bruneau, J. & Reverdin, C. (1999). Toroidal crystal spectrometer for time-resolved X-ray absorption diagnostic in dense plasmas. *Rev. Sci. Instrum.* **70**, 3314–3318.

Poletti, G, Orsini, F., Batani, D., Bernardinello, A., Desai, T., Ullschmied, J., Skala, J., Kralikova, B., Krousky, E., Pfeifer, M., Kadlec, C.H., Mocek, T., Preg, A., Renner, O., Cotelli, F., Lora Lami, C. & Zullini, A. (2004). Soft X-ray contact microscopy of nematode *Caenorhabditis elegans*. *Europ. Phys. J. D* **24**, 84.

Rosen, M.D., Hagelstein, P.L., Matthews, D.L., Campbell, E.M., Hazi, A.U., Whitten, B.L., Mac Gowan, B., Turner, R.E., Lee, R.W., Charatis, G., Busch, G.E., Shepard, C.L. & Rockett, P.D. (1985). Exploding-foil technique for achieving a soft X-ray laser. *Phys. Rev. Lett.* **54**, 106–109.

Rosmej, R., Faenov, A., Pikuz, T., Flora, F., Di Lazzaro, P., Bollanti, S., Lisi, N., Letardi, T., Reale, A., Palladino, L., Batani, D., Bossi, S., Bernardinello, S., Scafati, A., Reale, L., Zigler, A., Fraenkel, M. & Cowan, E. (1997). Inner-shell satellite transitions in dense short pulse plasmas. *J. Quant. Spec. Rad. Tran.* **58**, 859–878.

Rousse, A., Rischel, C. & Gauthier, J.-C. (2001). Femtosecond x-ray crystallography. *Rev. Mod. Phys.* **73**, 17–31.

Schollmeier, M., Prieto, G.R., Rosmej, F.B., Schaumann, G., Blazevic, A., Rosmej, O.N. & Roth, M. (2006). Investigation of laser-produced chlorine plasma radiation for non-monochromatic X-ray scattering experiments. *Laser Part. Beams* **24**, 335–345.

Stepanov, A., Starostin, A., Roerich, V., Makhrov, V., Faenov, A., Magunov, A., Pikuz, T., Skobelelev, I., Flora, F., Bollanti, S., Di Lazzaro, P., Lisi, N., Letardi, T., Palladino, L., Reale, A., Batani, D., Bossi, S., Bernardinello, A., Scafati, A., Reale, L., Osterheld, A. & Goldstein, W.

(1997). Modelling of the He-like magnesium spectral line radiation from the plasma created by XeCl and Nd-glass lasers. *J. Quant. Spec. Rad. Tran*. **58**, 937–952.

Turcu, E., Allot, R., Lisi, N., Batani, D., Bortolotto, F., Masini, A., Milani, M., Ballerini, M., Ferraro, L., Pozzi, A., Previdi, F. & Rebonato, L. (2004). An ensemble of new techniques to study soft X-ray induced variations in cellular metabolism. *Laser Part. Beams* **22**, 323–333.

Turcu, E., Maldonado, J.R., Ross, I., Shields, H., Trenda, P., Batani, D., Fluck, P. & Goodson, H. (1994*a*). Calibration of an excimer laser-plasma source for X-ray lithography. *Microelec. Engin.* **23**, 243–260.

Turcu, E., Tallents, G.J., Ross, I., Michette, A.G., Schulz, M., Meldrum, R.A., Wharton, C.W., Batani, D., Martinetti, M. & Mauri, A. (1994*b*). Optimisation of an excimer laser-plasma soft X-ray source for applications in biophysics and medical physics. *Phys. Medica* **X**, 93–99.

Warwick, P.J., Lewis, C.L.S., Kalachnikov, M.P., Nickles, P.V., Schnurer, M., Behjat, A., Demir, A., Tallents, G.J., Neely, D., Wolfrum, E., Zhang, J. & Pert, G.J. (1998). Observation of high transient gain in the germanium x-ray laser at 19.6 nm. *J. Opt. Soc. Am. B* **15**, 1808–1814.

Young, B.K.F., Osterheld, A.L., Price, D.F., Shepherd, R., Stewart, R.E., Faenov, A.Y.A., Magunov, A.I., Pikuz, T.A., Skobelev, I.Y.U., Flora, F., Bollanti, S., Di Lazzaro, P., Letardi, T., Grilli, A., Palladino, L., Reale, A., Scafati, A. & Reale, L. (1998). High-resolution X-Ray spectrometer based on spherically bent crystals for investigations of femtosecond laser plasmas. *Rev. Sci. Instrum.* **69**, 40–49.

Yuan, G., Kato, Y., Daido, H., Kodama, R., Murai, K. & Kagawa, T. (1996). Accurate wavelength determination of the lasing and non lasing lines in laser-produced germanium plasma. *Phys. Scripta* **53**, 197.

Zhang, J., Warwick, P.J., Wolfrum, E., Key, M.H., Danson, C., Demir, A., Healy, S., Kalantar, D.H., Kim, N.S., Lewis, C.L.S., Lin, J., Mac Phee, A.G., Neely, D., Nilsen, J., Pert, G.J., Smith, R., Tallents, G.J. & Wark, J.S. (1996). Saturated output of a Ge XXIII X-ray laser at 19.6 nm. *Phys. Rev. A* **54**, R4653–R4656.

https://doi.org/10.1017/S0263034607000080 Published online by Cambridge University Press